UNIVERSITY OF WASHINGTON

An Introduction to Nuclear Magnetic Resonance Imaging

Craig M. Dowell

Department of Physics, University of Washington, Seattle, WA 98195-1560

Abstract

An overview of the significant historical events in the development of MRI is presented. A summary of the equipment and results of Magnetic Resonance Imagine are presented. The underlying physics of Nuclear Magnetic Resonance are discussed, including the quantum mechanical and semi-classical views of spin and the statistical properties of bulk spin moments. The concepts of rotating reference frames and pulse sequences are developed, and methods of detection are examined. Spatial encoding is discussed and an example acquisition is illustrated. The concept of k-space is introduced and k-space traversal and two dimensional Fourier transforms are illustrated. Image quality issues are discussed and various MRI artifacts are shown.

1. INTRODUCTION

Nuclear Magnetic Resonance is a physical phenomenon. Under certain conditions, a charged particle can absorb energy from a surrounding magnetic field. When this absorption happens, the particle is said to be "in resonance" with the surrounding field. Felix Bloch and Edgar Mills Purcell demonstrated the nuclear magnetic resonance phenomenon in 1946 and were awarded the Nobel Prize in Physics for their work in 1952.

Over the next fifty years, the phenomenon of Nuclear Magnetic Resonance has been used to develop technologies for exploring the nuclear characteristics of atoms in various ways. From 1950 to 1970 a variety of NMR called Continuous Wave NMR was used. This method allowed an experimenter to probe resonances one frequency at a time, and was used for chemical and molecular analysis.

In 1971, Raymond Damadian showed that an NMR parameter, called the relaxation time, varied with the type of human tissue. This led him to begin developing Magnetic Resonance Imaging. Damadian was granted the first patent in the field of Magnetic Resonance Imaging.

An important advancement happened in 1973 when Paul Lauterbur first demonstrated an image of two test tubes of water correctly oriented in space. Peter Mansfield further developed Lauterbur's work and showed how the MRI signals could be mathematically analyzed. In 1975, Richard Ernst proposed using frequency encoding and Fourier transforms – a methodology which "transformed" the field and led to modern FT-NMR.

In 1980, William Edelstein first demonstrated imaging the human body and Kurt Wüthrich used NMR to find the 3-D structure of proteins. In 2005, only 25 years later, there are approximately 5,000 MRI machines in the United States alone, and some 60,000,000 clinical MRI scans are done here every year.

There have been a number of Nobel Prizes awarded for work in NMR. Bloch and Purcell shared the Nobel Prize for physics in 1952 for their discovery of NMR. In 1991, Ernst earned a Nobel in Chemistry for the development of the methodology of high resolution nuclear magnetic resonance spectroscopy. The 2002 Nobel Prize for chemistry went to Kurt Wüthrich for development of NMR spectroscopy. Paul Lauterbur and Peter Mansfield shared a Nobel Prize in Medicine in 2003 for demonstrating that gradient fields and Fourier transforms could be used to create two-dimensional pictures.

The most well known application of NMR is in Nuclear Magnetic Resonance Imaging. NMRI is a technique for producing cross-sectional images of the interior of the human body without x-rays. NMRI uses Nuclear Magnetic Resonance to extract information about the atomic makeup of the body which is then processed to create images. When you go to the doctor, he will tell you to have an MRI done, not an NMRI, though. People are put off by the word Nuclear and it is typically not used.

MRI, in essence, asks the following question: "If the body is divided up into a large number of tiny volumes, what kind of tissue is there in each of those volumes"? Different materials will have different characteristics and MRI will discern those differences and visualize them. The result is a detailed map of information about the material in each tiny volume.

Images are usually produced of various virtual slices through the body. The different structures are typically displayed as various shades of gray. Figure 1 shows the kind of image that is possible with a commercially available MRI system, the Achieva 1.5T, manufactured by Philips Medical Systems.

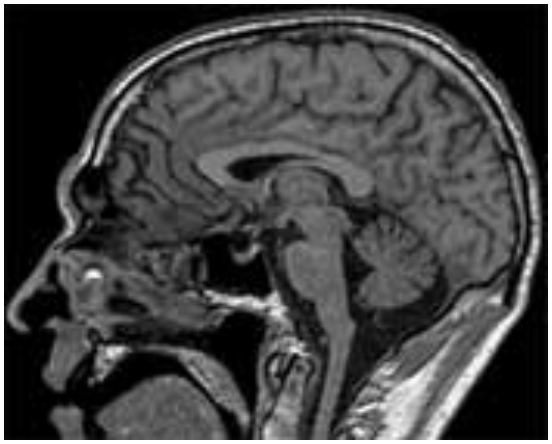

FIG. 1: An MRI Image of the Human Head. Taken with a Philips Achieva 1.5T

MRI systems, since they all exploit the same underlying physics, have the same basic form. When one looks at an MRI system, the most obvious feature is the magnet – a very large superconducting magnet.[1] There is a hole in the magnet, called the bore, through which a patient's body is moved on a special table. Figure 2 shows two commercially available MRI systems.

[1] The 1.5T designation of the Philips Achieva signifies a 1.5 Tesla magnetic field. For purposes of comparison, one Tesla is 10,000 Gauss. Watches, paper clips, keys and even stethoscopes can become dangerous projectiles around these devices when they are operating. There have been cases of vacuum cleaners and even oxygen tanks being pulled into the bore of an operating MRI magnet.

FIG 2: Philips Achieva (left) and Siemens Avanto (right) MRI Systems.

The large superconducting magnet produces a uniform and static magnetic field. There are also gradient magnets and RF coils involved in producing the data required for the images. The gradient magnets allow the MRI machine to create axial, sagittal or coronal visualizations. If you imagine a person on the table, a sagittal slice of the head would be, for example, a slice from the the tip of the nose to the back of the skull, resulting in an image with the head in profile. Figure 1 is a sagittal image of the head. An axial image would result in circular sections from the top of the head down toward the chin, as illustrated in Figure 3 (a). A coronal image results in a slice from ear to ear, illustrated in Figure 3 (b).

(a) 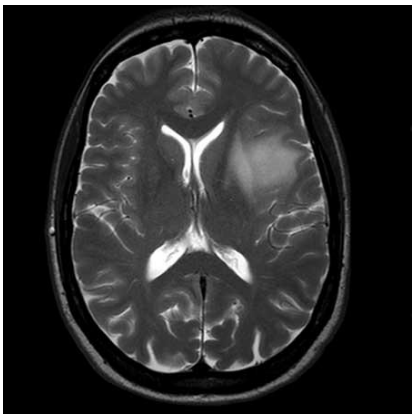 (b) 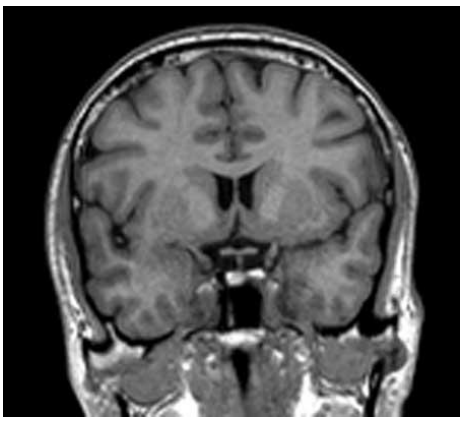

FIG 3: Axial (a) and Coronal (b) Images of the Human Head

Another important piece of equipment for an MRI system is the coil. The coil is used to excite the body with RF energy and also to measure the response. There are different coils for different uses. Figure 4 shows a head and neck coil just about to enter a Philips Achieva 1.5T through the magnet bore. In the case of the pediatric head and neck coil shown in the figure, a child's head would be inserted in the cage-like coil and the platform moved so that the head is in the center of the bore.

FIG 4: Pediatric Head and Neck Coil for Philips Achieva 1.5T.

The human body is composed of billions of atoms, each of which has a nucleus. Many varieties of these nuclei act like magnets and therefore have magnetic moments. The static magnetic field causes the nuclei to align with the field, in one way or the other depending on their energy. Lower energy protons align themselves with the magnetic field, and higher energy protons align themselves against the field. There will always be a larger number of lower energy protons than higher. Instead of sitting there quietly, the nuclei precess, or rotate around the field in the same way a gyroscope would move in a gravitational field. The stronger the field, the better aligned are the little magnets, just like a rapidly spinning gyroscope.

An RF field is applied to the subject, using the RF coil, which causes the lower energy protons to absorb energy, "flip," and begin precessing in the opposite direction. When the RF field is turned off, the protons begin to "relax" back to their natural alignment with a small excess of lower energy protons precessing aligned with the field. When the protons relax, they emit the energy that they absorbed from the RF field, and the coil (now functioning as a detector) picks up that energy. The electromagnetic signals corresponding to the released energy are captured by the MRI system and then processed by a computer in order to construct the final MRI image.

2. THE UNDERLYING PHYSICS

MRI is essentially a two-step process that works because we are able to observe the way protons in a person's body respond to magnetic fields. In the first step, we manipulate the spin orientations of the protons in the body; and in the second step, we measure changes in those orientations with a detector. Although the magnetic field of each proton is tiny, there are many Avogadro numbers of them in the body, and we can measure the sum of all of those fields.

2.1 QUANTUM MECHANICAL SPIN

In classical mechanics, an object can undergo two types of angular momentum: The first type, orbital angular momentum ($L = r \times p$), is associated with motion of the center of mass of the object around some point – like the Earth orbiting around the sun. The second type, spin ($S = I\omega$), is associated with the motion of the object around its center of mass – like the Earth spinning on its axis.

In quantum mechanics, elementary particles carry a third type of angular momentum, called intrinsic angular momentum (S). This has nothing to do with motion in space, but is somewhat analogous to classical spin and so the same term is used. Every kind of particle has a specific value of spin which never changes. For example, electrons, neutrons and protons have spin ½, while photons have spin 1. We will be interested in spin ½ in this instance, and particularly how particles with spin react to magnetic fields.

The Schrödinger equation, models this quantum mechanical behavior:

$$i\hbar \frac{\partial \Psi}{\partial t} = H\Psi \, .$$

It can be solved by separation of variables. The solution constructs simultaneous eigenfunctions of three commuting operators, H, L^2 and L_z:

$$H\Psi = E\Psi, \quad L^2\Psi = \hbar^2 l(l+1)\Psi, \quad L_z\Psi = \hbar m\Psi \, .$$

Here, the variable l is the azimuthal quantum number. Recall that the azimuthal quantum number manifests itself in the shape of an orbital. The m is the magnetic quantum number which represents the orientation of the angular momentum. The algebraic theory of spin is exactly the same as that of orbital angular momentum, so we can write,

$$H\Psi = E\Psi, \quad S^2\Psi = \hbar^2 s(s+1)\Psi, \quad S_z\Psi = \hbar m\Psi \, .$$

We usually write this is Dirac notation

$$H|s\ m\rangle = E|s\ m\rangle, \quad S^2|s\ m\rangle = \hbar^2 s(s+1)|s\ m\rangle, \quad S_z|s\ m\rangle = \hbar m|s\ m\rangle$$

Where s is the spin (½) and m is either (+½ or –½). Thus the orientation takes on two values, which we interpret as parallel to an axis or antiparallel. For NMR we usually restrict ourselves to the Z-axis. For spin ½ particles we then have two eigenstates,

$$\left|\frac{1}{2}\ \left(+\frac{1}{2}\right)\right\rangle, \text{ which we call spin up, and}$$

$$\left|\frac{1}{2}\ \left(-\frac{1}{2}\right)\right\rangle, \text{ which we call spin down.}$$

The general state of a spin- ½ particle can be expressed as a two element matrix called a spinor:

$$\chi = \begin{pmatrix} a \\ b \end{pmatrix} = a\chi_+ + b\chi_-,$$

Where χ_+ represents spin up and χ_- represents spin down. In matrix representation,

$$\chi_+ = \begin{pmatrix} 1 \\ 0 \end{pmatrix} \text{ and } \chi_- = \begin{pmatrix} 0 \\ 1 \end{pmatrix}.$$

In the matrix representation, spin operators also become matrices, and the matrix we will be primarily concerned about here will be the S_z matrix,

$$S_z = \frac{\hbar}{2}\begin{bmatrix} 1 & 0 \\ 0 & -1 \end{bmatrix}.$$

A spinning charged particle acts like a magnetic dipole. The particle's magnetic dipole moment ($\vec{u}$) is proportional to its spin angular momentum,

$$\vec{u} = \gamma\vec{S},$$

and the proportionality constant (γ) is called the gyromagnetic ratio.

A magnetic dipole experiences a torque, ($\vec{u} \times \vec{B}$) in a magnetic field ($\vec{B}$). This torque is in a direction that tends to line the dipole up parallel to the magnetic field. The energy associated with this torque is,

$$E = -\vec{u} \bullet \vec{B}$$

And therefore the Hamiltonian is,

$$\mathcal{H} = -\gamma \vec{B} \bullet \vec{S}$$

If we consider a proton in a uniform magnetic field $\vec{B} = B_0 \hat{z}$ along the z-axis, the matrix representation of the Hamiltonian will be

$$\mathcal{H} = -\gamma B_0 S_z = -\gamma B_0 \frac{\hbar}{2}\begin{bmatrix} 1 & 0 \\ 0 & -1 \end{bmatrix}.$$

The Hamiltonian is time-independent, so the general solution to the time-dependent Schrödinger equation is,

$$i\hbar \frac{d}{dt}\chi = \mathcal{H}\chi .$$

We can express the solution in terms of stationary states,

$$\chi\ t\ = a\chi_+ e^{-i\frac{E_+ t}{\hbar}} + b\chi_+ e^{-i\frac{E_- t}{\hbar}}.$$

Since $\mathcal{H}\left|s\ m\right\rangle = E\left|s\ m\right\rangle$,

$-\gamma B_0 \frac{\hbar}{2}\begin{bmatrix} 1 & 0 \\ 0 & -1 \end{bmatrix}\begin{bmatrix} 1 \\ 0 \end{bmatrix} = -\gamma B_0 \frac{\hbar}{2}\begin{bmatrix} 1 \\ 0 \end{bmatrix}$ implies that for χ_+ the energy $E_+ = -\gamma B_0 \frac{\hbar}{2}$, and

$-\gamma B_0 \frac{\hbar}{2}\begin{bmatrix} 1 & 0 \\ 0 & -1 \end{bmatrix}\begin{bmatrix} 0 \\ 1 \end{bmatrix} = +\gamma B_0 \frac{\hbar}{2}\begin{bmatrix} 0 \\ 1 \end{bmatrix}$ implies that for χ_- the energy $E_- = +\gamma B_0 \frac{\hbar}{2}$.

Putting this together, we find

$\chi\ t\ = a\chi_+ e^{-i\frac{-\gamma B_0 \frac{\hbar}{2} t}{\hbar}} + b\chi_+ e^{-i\frac{+\gamma B_0 \frac{\hbar}{2} t}{\hbar}}$, which we can write as $\chi\ t\ = \begin{pmatrix} ae^{\frac{i\gamma B_0 t}{2}} \\ be^{\frac{-i\gamma B_0 t}{2}} \end{pmatrix}$.

With a little foreknowledge, we can write $a = \cos(\frac{\alpha}{2}), \quad b = \sin(\frac{\alpha}{2}),$ and calculate the expectation values of S_x, S_y, and S_z.

$$\langle S_z \rangle = \begin{bmatrix} \cos(\frac{\alpha}{2})e^{\frac{-i\gamma B_0 t}{2}} & \sin(\frac{\alpha}{2})e^{\frac{-i\gamma B_0 t}{2}} \end{bmatrix} \frac{\hbar}{2} \begin{bmatrix} 1 & 0 \\ 0 & -1 \end{bmatrix} \begin{bmatrix} \cos(\frac{\alpha}{2})e^{\frac{i\gamma B_0 t}{2}} \\ \sin(\frac{\alpha}{2})e^{\frac{-i\gamma B_0 t}{2}} \end{bmatrix} = \frac{\hbar}{2}\sin\ \alpha\ \cos\ \gamma B_0 t$$

$$\langle S_y \rangle = \begin{bmatrix} \cos(\frac{\alpha}{2})e^{\frac{-i\gamma B_0 t}{2}} & \sin(\frac{\alpha}{2})e^{\frac{-i\gamma B_0 t}{2}} \end{bmatrix} \frac{\hbar}{2} \begin{bmatrix} 0 & -i \\ i & 0 \end{bmatrix} \begin{bmatrix} \cos(\frac{\alpha}{2})e^{\frac{i\gamma B_0 t}{2}} \\ \sin(\frac{\alpha}{2})e^{\frac{-i\gamma B_0 t}{2}} \end{bmatrix} = -\frac{\hbar}{2}\sin\ \alpha\ \sin\ \gamma B_0 t$$

$$\langle S_z \rangle = \begin{bmatrix} \cos(\frac{\alpha}{2})e^{\frac{-i\gamma B_0 t}{2}} & \sin(\frac{\alpha}{2})e^{\frac{-i\gamma B_0 t}{2}} \end{bmatrix} \frac{\hbar}{2} \begin{bmatrix} 1 & 0 \\ 0 & -1 \end{bmatrix} \begin{bmatrix} \cos(\frac{\alpha}{2})e^{\frac{i\gamma B_0 t}{2}} \\ \sin(\frac{\alpha}{2})e^{\frac{-i\gamma B_0 t}{2}} \end{bmatrix} = \frac{\hbar}{2}\cos\ \alpha$$

From the expression $\langle S_z \rangle = \frac{\hbar}{2}\cos\ \alpha$ we can infer that $\langle S \rangle$ is tilted away from the z-axis at a constant angle α. From the expressions for $\langle S_z \rangle$ and $\langle S_z \rangle$ we infer that the spin vector precesses around the z-axis at a frequency $\omega = \gamma B_0$. This frequency is called the Larmor frequency and it is dependent on the gyromagnetic ratio of the particle and on the magnetic field.

We saw that the energy of the quantum state with S_z parallel to the magnetic field is

$$E_+ = -\gamma B_0 \frac{\hbar}{2},$$

Which is a lower energy than

$$E_- = +\gamma B_0 \frac{\hbar}{2}.$$

This is an example of the Zeeman effect. Whenever an atom is placed in a uniform external magnetic field, the energy levels are shifted. We have calculated the difference between the energies in this case to be $\gamma B_0 \hbar$. This is equal to $\omega\hbar$ since $\omega = \gamma B_0$. In the same way that an atom can absorb or emit a photon and change energy state, a particular proton can be induced to change its magnetic field alignment if it receives an amount of energy equivalent to $\omega\hbar$ where ω is the Larmor frequency. This is nuclear magnetic resonance.

2.2 MACROSCOPIC SPIN

When making the transition from the quantum world to the macroscopic world, we begin to look at the average orientations of the spins of Avogadro numbers of protons. One could imagine that all of the protons the found in a human body would simply fall into the lowest energy state with their magnetic moments aligned with the field. If this were the case we would see a very large effective magnetic moment. The reality is a bit more subtle.

There is a trade-off between the tendency of a spin system to remain aligned with the magnetic field, and the ability of the system to gain energy. Some fraction of the protons in the body will gain energy from thermal contact with their surroundings and change orientations to the higher energy state – that with the spin aligned antiparallel to the magnetic field. The number that do is related to the Boltzmann factor, which is the probability that a given system will be found at a particular energy. This factor is,

$$P(E) = e^{-\frac{E}{kT}}.$$

Previously, we calculated E_+ (spin up, aligned parallel to the field, lower energy) and E_- (spin down, antiparallel to the field, higher energy). If we plug those numbers in, we can find a ratio of probabilities that a sample of protons will be in a particular state,

$$\frac{P(E_+)}{P(E_-)} = \frac{e^{\frac{\gamma\hbar B_0}{2kT}}}{e^{-\frac{\gamma\hbar B_0}{2kT}}}.$$

Using $\gamma = 42.58\,MHz/T$ (hydrogen), $B_0 = 1.5T$ (the magnetic field in the Philips Achieva 1.5T), and T=295K (room temperature – 72º F) we find

$$\frac{P(E_+)}{P(E_-)} \approx \frac{1.00000520}{0.99999480}.$$

There is an almost vanishingly small preference of protons to be in the aligned state. The vast majority of protons cancel each others magnetic moments. The ratio above may be barely above unity, but Avogadro's number is big. There will still be on the order of 10^{18} protons per gram of hydrogen that align with the static field. This is called the spin excess and provides a macroscopic magnetization that can be detected.

2.3 ROTATING MAGNETIC FIELDS

Quantum mechanically, the MRI system needs to be able to add energy to the protons of a subject in units of $\omega\hbar$. This implies a rotation of a magnetic field at a frequency $\omega = \gamma B_0$

A rotating magnetic field may be implemented using two perpendicular coils with sinusoidal currents in each coil separated in phase by 90º. One of the coils drives the x-component of the field, and the other coil drives the y-component. Looking at Figure 5, you can see that if a cosine wave generates the x-component, and a sine wave generates the y-component, the result is a magnetic field vector rotating in the x-y axis.

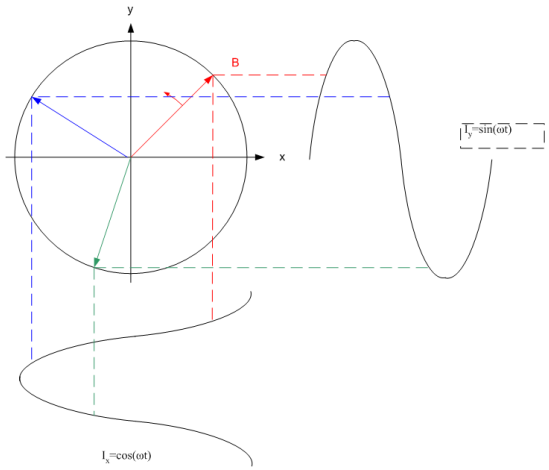

FIG 5: Rotating Magnetic Field

If we were to add a z-axis to Figure 5, it would sprout out of the page. We use these coordinates to define a laboratory frame with the z-axis running down the bore of the superconducting magnet of the MRI machine. Figure 6 shows how this lab frame would look.

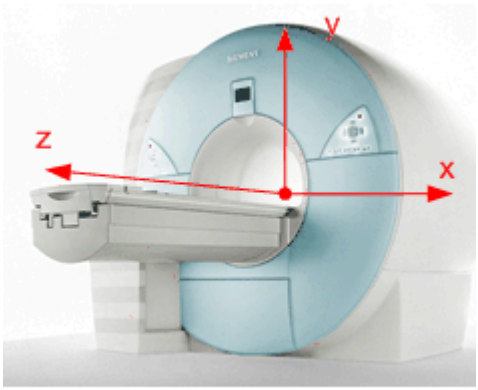

FIG 6: The Laboratory Coordinate System

2.4 ROTATING REFERENCE FRAMES

If we take a semiclassical view of a subject immersed in the large static magneitic field of an MRI machine, we will see a macroscopic magnetic dipole moment $\vec{u} = \gamma \vec{J}$ which is a result of the sum of all of the quantum mechanical magnetic dipole moments $\vec{u} = \gamma \vec{S}$ of the subject. This macroscopic magnetic dipole moment will precesss around the z-axis of our laboratory frame at a frequency $\omega = \gamma B_0$. We have proposed another magnetic field (usually called the RF field) designated B_1 which is rotating around the z-axis in the x-y plane at the same frequency, as illustrated in Figure 7. Consider what this situation would look like in a frame where the x-y plane is also rotating at $\omega = \gamma B_0$. Both B_0 and B_1 would be rotating at the same rate and would be *static* in this reference frame.

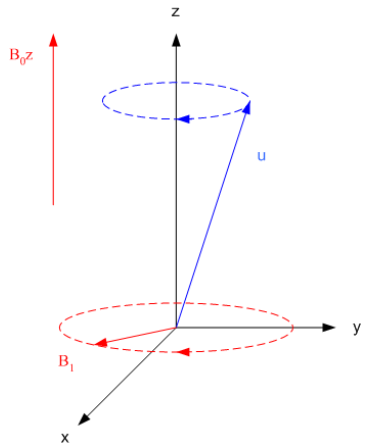

FIG 7: The Magnetic Fields and the Dipole Moment

This rotating reference frame turns out to be very useful for understanding what is happening in MRI systems. The equation of motion for the dipole moment in the laboratory frame is,

$$\frac{d\vec{u}}{dt} = \vec{u} \times \gamma \left[\vec{B}_0 + \vec{B}_1 \;\; t \;\; \right].$$

If we take H_1 along the x-axis, and transform into the rotating frame, the equation of motion becomes,

$$\frac{\delta \vec{u}}{\delta t} = \vec{u} \times \gamma \left[\left(B_0 - \frac{\omega}{\gamma} \right) \hat{z} + B_1 \hat{x}' \right].$$

We then define an effective magnetic field in this frame,

$$B_{eff} = \left(B_0 - \frac{\omega}{\gamma} \right) \hat{z} + B_1 \hat{x}',$$

And discover that the cosine of the angle between the center of precession and the effective field is

$$\cos\ \theta\ = \frac{B_0 - \frac{\omega}{\gamma}}{B_{eff}}.$$

The angle θ in the macroscopic rotating frame view corresponds to the angle α in the quantum mechanical treatment we developed previously. If we are operating at $\omega = \gamma B_0$, the term in parentheses in B_{eff} above drops out and the magnetic moment sees a torque of,

$$\vec{u} \times \gamma B_1 .$$

A magnetic moment that is initially parallel to the static field (in the z-axis) will be caused to rotate in the z-y plane at a frequency of $\omega = \gamma B_1$ as illustrated in Figure 8. (N.B. the orientation of the axes in the figure, with the z-axis vertical).

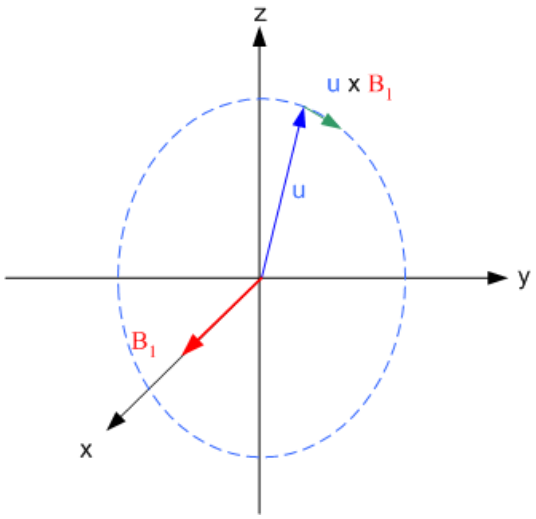

FIG 8: The Magnetic Dipole Moment Rotated by the Torque of the RF Field

In the jargon of MRI systems, if the rotating magnetic field is turned on for a time corresponding to a rotation of $\vec{u}$ around a quarter of the circle in Figure 8 and then turned off, it is called a $\pi/2$ pulse. This is because $\vec{u}$ will rotate $\pi/2$ radians in that time . Figure 9 shows the effect of a pulse of this type on the macroscopic magnetic dipole moment as viewed in the lab frame. Think of the tip of the vector as initially precessing tightly around the z-axis under the influence of the strong static magnetic field B_0.

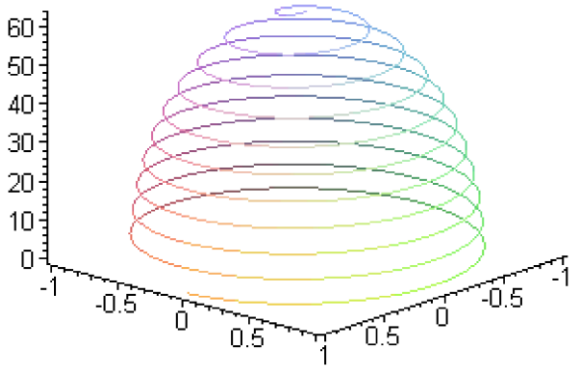

FIG 9: Effect of $\pi/2$ Pulse in Lab Frame

When the rotating magnetic field is turned on, a torque is applied to $\vec{u}$ which tends to rotate its precession intoe x-z plane. Since $\vec{u}$ is precessing, it *spirals* down to the x-z plane.

2.5 RELAXATION

Once a proton spin is manipulated to cause it to precess around the z-axis in the x-y plane, as a result of a $\pi/2$ pulse for example, it does not remain in that state. The proton spins want to return to their equilibrium value. This process will leave us back where we started with a spin excess number of protons aligned with the static magnetic field as predicted by the ratio of Boltzmann factors.

A π pulse (just continue a $\pi/2$ pulse until the precession moves through the x-z plane, and past, until the magnetic dipole precesses around to the –z axis) will add enough energy to the protons in the body to change the quantum state of each one of the lower energy protons involved in the spin excess from E_+ (the lower energy spin ½ state) to E_- (the higher energy spin –½ state).

This energy is returned during relaxation. The relaxation is exponential and caused by several mechanisms. The time constant describing the relaxation is called the *Combined Relaxation Time* and is designated T_2^*.

One of the mechanisms responsible for returning energy is related to the local environment of the protons. The local environment is called the "lattice" (since most of the early experimenters in Nuclear Magnetic Resonance were solid-state physicists). The excess energy above the ground state that was acquired by each proton during the rotating field pulse is returned to its surroundings. This mechanism is called spin-lattice relaxation and the corresponding time constant (T_1) is called the spin-lattice relaxation time – the time it takes to reduce the *longitudinal* magnetization by a factor of e:

$$M_z\ t\ = M_z\ t_0\ e^{-\frac{t-t_0}{T_1}} + M_0\left(1-e^{-\frac{t-t_0}{T_1}}\right) \qquad \text{B} \parallel \hat{\text{z}}\ .$$

The spin-lattice relaxation time is experimentally determined. Some typical values for various human tissues are shown in Table 1.

Another mechanism driving relaxation is the spin-spin relaxation. This mechanism is driven by *local* inhomogeneities in the magnetic field. Different values of the local magnetic field lead to different precession frequencies. For example, electrons can shield nuclei from the ambient magnetic field.[2] This difference in magnetic field leads to the individual spins gradually "dephasing" and resulting in a reduction in the total *transverse* magnetization vector to its equilibrium value of 0. This is an exponential function, with T_2 being the time it takes to reduce the transverse magnetization by a factor of e:

$$\vec{M}_{\perp}(t) = \vec{M}_{\perp}(0)e^{-\frac{t}{T_2}}.$$

Table 1 also shows typical values for T_2.

Tissue	T_1 (ms)	T_2 (ms)
Gray Matter	950	100
White Matter	600	80
Muscle	900	50
Cerebrospinal Fluid	4500	2200
Fat	250	60
Arterial Blood	1200	200
Venous Blood	1200	100

Table 1: Approximate values of relaxation parameters T_1 and T_2 at B_0 = 1.5T, T = 37º C

There is an additional dephasing of the spins due to *external* field inhomogeneities and is defined to be

$$T_2^{'} = \gamma \Delta B_0 .$$

The combined relaxation time is defined as

$$\frac{1}{T_2^*} = \frac{1}{T_1} + \frac{1}{T_2} + \frac{1}{T_2^{'}}$$

2.7 DETECTION

In the previous sections we have seen how the MRI system manipulates the magnetic dipole moments of the body. The result of this process is to cause the magnetic dipole

[2] This is, in fact, the basis for NMR Spectroscopy. The structure of nearby electrons affects the local environment of the protons allowing us to discern the 3-D structure of the surrounding elements.

moment of the body to precess in certain orientations. Once the driving force is removed, the dipole moments continue to precess and produce their own changing magnetic fields. It is the change in those fields over time which allows us to observe the Nuclear Magnetic Resonance and its decay.

According to Faraday's law, an electric field will be generated by a changing magnetic field:

$$\nabla \times \vec{E} = -\frac{\partial B}{\partial t}.$$

More to the point in this case is the "universal flux rule," which says that an electromotive force will be generated in any coil through which a magnetic flux passes:

$$\mathcal{E} = -\frac{d\Phi}{dt}.$$

Consider first a hypothetical macroscopic bar magnet spinning in the vicinity of a coil, as illustrated in Figure 11. This is simply an electric generator. Now imagine replacing the magnet with the precessing magnetization of the body caused by the actions of the external static field and the rotating field.

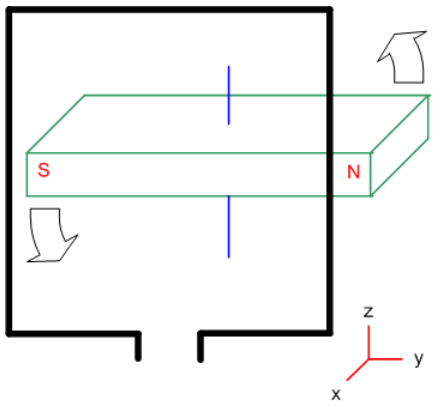

FIG 11: An Electric Generator

This situation is illustrated in Figure 12. This illustration shows a red magnetic field vector, B(t), rotating in the x-y plane representing the precessing proton spins. A (thick black) coil is shown placed in the x-z plane with its center at the origin to detect the changing field.

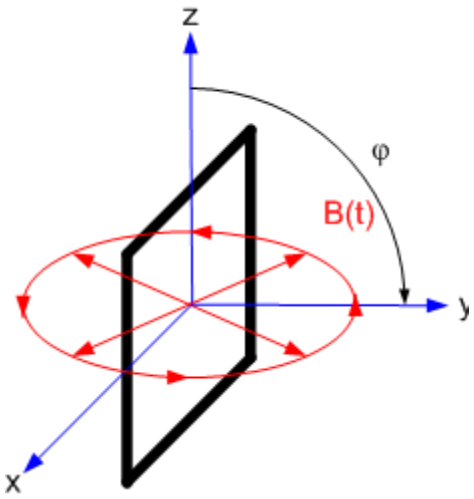

FIG 12: A Stylized MRI Detector

The rotating magnetic field should look familiar; it is just like the field applied to manipulate the precession of the proton spins, but here it is due to the proton spins themselves.

The rotating magnetic field caused by the macroscopic moment could be described by,

$$\vec{B}\ t\ = B\ \cos\omega t\hat{x} + \sin\omega t\hat{y}\ \ .$$

Taking into account the angle φ (which corresponds to the angle of precession; through which the torque of the rotating RF field caused the spins to rotate; and also through which the change in energy due to relaxation will cause the spins to rotate the other way), we have,

$$\vec{B}\ t\ = B\sin\phi\ \cos\omega t\hat{x} + \sin\omega t\hat{y}$$

We can then find the flux through the coil is found by the universal flux rule,

$$\Phi = \int_{\text{Coil Area}} \vec{\mathrm{B}} \bullet d\vec{S}\ ,$$

where $d\vec{S}$ is $dx\ dz\ \hat{y}$. If we imagine the field is constant over the coil at any particular time ($d\varphi/dt$ is constant – we can do this since the relaxation time is measured in hundreds of milliseconds, and the RF field is measured in megahertz), we find,

$$\Phi = \int_{-L/2}^{L/2} dx \int_{-L/2}^{L/2} dz\ \ \hat{y} \bullet B\ \ t\ \ = L^2\ \ \hat{y} \bullet B\ \ t\ \ \ = L^2 B\sin\omega t\sin\phi\ .$$

We differentiate to find the induced emf:

$$\mathcal{E} = -\frac{d}{dt} L^2 B \sin\omega t \sin\phi = -L^2 B\omega \cos\omega t \sin\phi \,.$$

Imagine that we are applying an RF pulse to a subject. Initially the magnetic dipole moment of the subject is precessing tightly around the z-axis. In this case, $\sin\phi = 0$ and no EMF is induced in the coil. Figure 13 shows how a response (the induced EMF in the coil) to a 2π pulse might be seen.

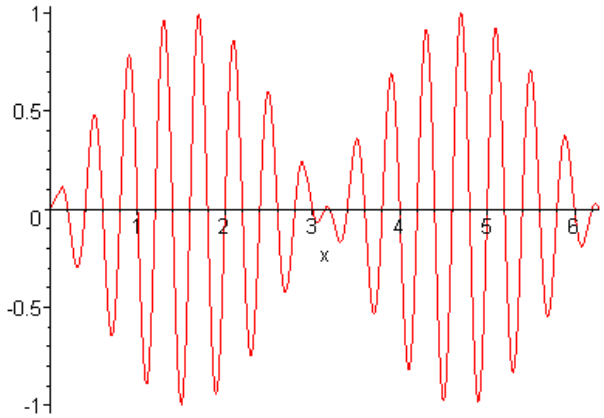

FIG 13: A Two Pi Pulse

The signal grows from zero to a first maximum when the magnetic field is rotating in the x-y plane. At this point, $\phi = \pi/2$ we have applied a $\pi/2$ pulse. The signal then decreases until the spins are precessing in the –y axis. Here, we have applied a π pulse. As we continue driving the spins, we rotate on around and see another peak which corresponds to a $3\pi/2$ pulse, and then another reduction as the spins come back around to a 360º rotation.

If we were to suddenly turn off the driving rotating magnetic field at the $\pi/2$ point, the relaxation process would begin and we would see an exponential decay of the signal, with the time constant determined by T_2^* as described above. Figure 14 shows what the response to a $\pi/2$ pulse, followed by a relaxation might look like. The decay portion of the signal envelope is known as the Free Induction Decay (FID).

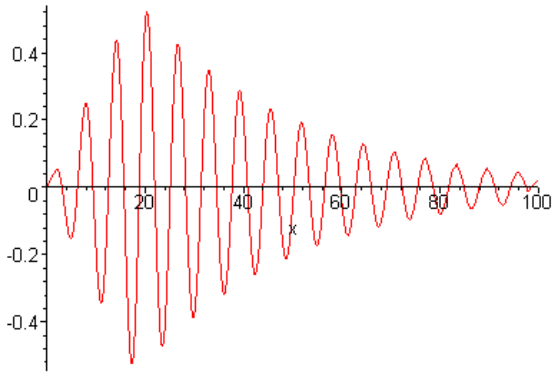

FIG 14: Free Induction Decay Following a Pi/2 Pulse

The signal shown in Figure 14 is typically demodulated (in the sense of rectifying and filtering) and displayed as an exponentially decaying curve from the point at which the driving field is removed. Figure 15 shows what a typical demodulated FID signal could look like. This is also how the FID signal would appear in the rotating reference frame, by the way.

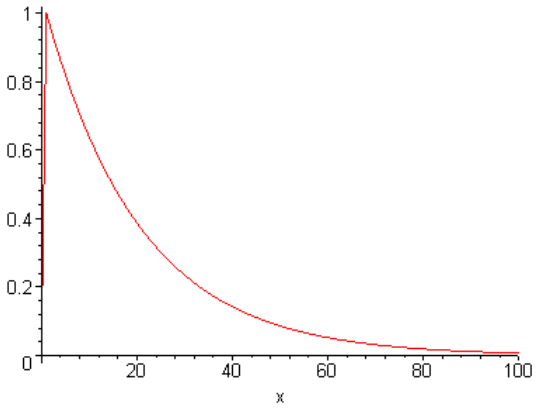

FIG 15: Demodulated Free Induction Decay Following a Pi/2 Pulse

2.8 SPIN ECHO

The spin echo method is based on the application of two RF pulses. The first is a $\pi/2$ pulse, and the second is a refocusing π pulse. After the initial $\pi/2$ pulse, the spins at different positions begin to dephase as they experience different local field strengths. After a time, a π pulse is applied. This pulse is of the same duration as the $\pi/2$ pulse but at twice the amplitude. This has the effect of changing all of the spins that had dephased by $-\phi$ into $+\phi$ and vice versa.

The local fields have not changed during this process, and so the spins that were dephasing in a $-\phi$ direction continue to do so. However, we changed the sign of the

phase with the π pulse. This means that the spins that are headed downward were reversed to have a $+\phi$ and are now headed back down toward zero phase. The dephasing process has been reversed and the spins will drift into resonance. This results in reforming, or "echo" of the peak shown in Figure 14.

The characteristics of the spin echo envelope are directly related to the spin-spin relaxation properties of the substance, and give us an indication of T_2 (see Table 1). If use the FID to determine T_1, and Spin Echo to determine T_2, we can be more precise in identifying substances in the body. For example, according to Table 1, venous and arterial blood both exhibit T_1 times of 1200 mS. However, arterial blood has a T_2 time which is twice that of venous blood.

2.9 PULSE SEQUENCES

An MRI machine will make many measurements of the FID, the spin echo, and other properties during an examination of a subject. The arrangement of stimuli (gradients, RF pulses – the rotating magnetic field) and measurements are arranged in a *Sequence Diagram*. An example of the most basic sequence is shown in Figure 16.

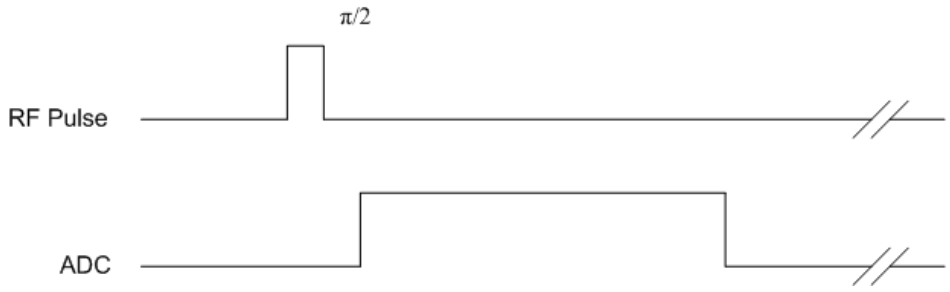

FIG 16: A Basic MRI Pulse Sequence Diagram

Here a $\pi/2$ pulse is applied, and the FID is measured by enabling an Analog to Digital Converter (ADC) which converts the FID signal into a numerical representation. It is assumed that the pulse sequence repeats a large number of times.

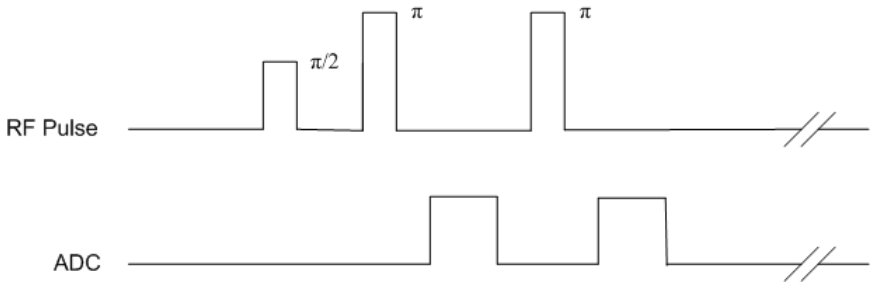

FIG 17: An Example Spin Echo Measurement Sequence Diagram

Figure 17 shows a pulse sequence which would detect spin echoes. Note that, the π pulse is shown with the same pulse width as the $\pi/2$ pulse but with twice the amplitude. The ADC is enabled during the period where the spins are expected to rephrase and produce the spin echo.

3. VISUALIZATION

The object of the MRI is to determine the presence of a particular nuclear species at each voxel[3] under examination. The Larmor frequency at that point depends on the species that exists there, specifically on the gyromagnetic ratio of the nucleus, and the magnetic fields present, of both local and external origin.

One can imagine that one way to determine the spin response of a subject is to apply a number of narrow-band RF pulses, each at specific frequencies. This arrangement is analogous to the way one would measure the frequency response of a stereo system. You could send a known signal of 50 Hz, for example, through the system, and measure the response at that frequency. You could increase the frequency, in small steps, and repeat the measurements throughout the range of frequencies of interest. You might find a frequency response (if you are lucky enough to own McIntosh equipment) like that shown in Figure 18.

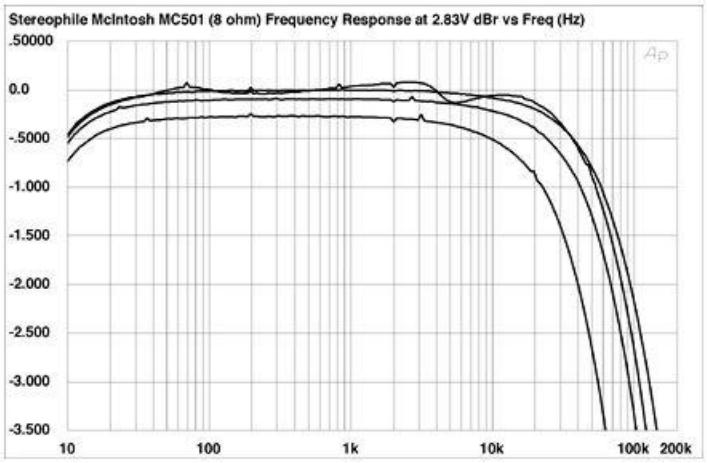

FIG 18: Frequency Response of a Stereo Amplifier

This would be a time consuming process, though. You could accomplish the same thing in one measurement if you applied a broadband signal, and made all of your measurements all at once. This is possible, and the key is to drive the system using a square wave and to use Fourier Transforms to reconstruct the response to each frequency component.

Recall that a square wave can be constructed from the infinite series,

$$y = \sin(x) + \frac{1}{3}\sin(3x) + \frac{1}{5}\sin(5x) + \cdots$$

[3] A voxel is a volume element, in the same spirit as a pixel is a picture element.

and is typically illustrated by a plot that looks something like Figure 19.

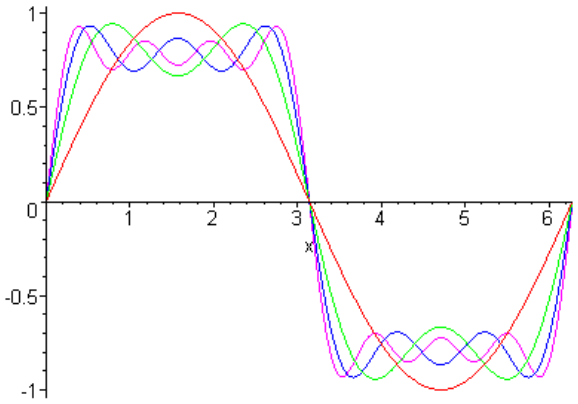

FIG 19: Square Wave Expressed as Sum of Sine Waves

A square wave can be viewed as being composed of an infinite number of sine waves. If we apply a square wave input to our stereo amplifier, and measure the voltage versus time response to that square wave, we could in principle figure out how the system responded to each of the sine waves that made up the square wave. This is the essence of what the MRI system will do.

3.2 SPATIAL ENCODING

As mentioned in the introduction, there are three gradient magnets in an MRI system. The purpose of the three gradient magnets is to provide spatial encoding for the points in the body at which resonance occurs.

The Larmor frequency of a spin will be linearly proportional to its position on the z-axis if the static field is augmented with a linearly varying field:

$$\omega = \gamma(B_0 + zB_g)\,.$$

The use of a magnetic field gradient to establish a relation between the spatial position of a spin and its precession rate is called frequency encoding.

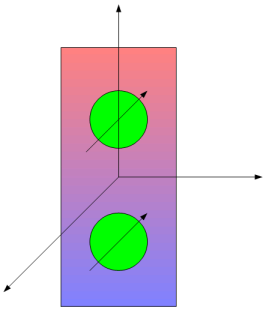

FIG 20: Protons Precessing in a Gradient

Consider a simple example of two protons near each other on the z-axis, as shown in Figure 20. The gradient causes the magnetic field to be slightly higher at the upper proton (shown as a red area in the figure).The proton in the blue area is in a magnetic field slightly lower than that of the red proton. The result is that proton in the red area will precess slightly faster than the proton in the blue area.

The resulting magnetic field produced by the rotating proton spins is the superposition of the two precession rates. Since the two frequencies are not identical they will beat against each other, as shown in Figure 21.

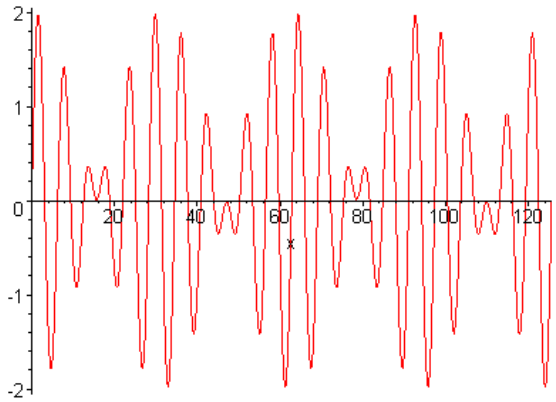

FIG 21: Precession Beats

The beat frequency will be proportional to the spatial separation between the spins since the precession rates are proportional to the separation. Therefore, *the resulting waveform encodes spatial information about the sample.* If we were to analyze the frequency domain representation of this signal we would see a peak corresponding to each of the original frequencies, the sum of the frequencies and the difference. The peak which corresponds to the difference frequency encodes the distance between the spins.

Now, consider applying a gradient field to a thin cylinder of some material we wish to image instead of just the two protons. The gradient will cause the protons in the cylinder to precess at a rate which is proportional to their position on the axis of interest – call this the z-axis.

After the application of a gradient field, the protons in the material at a position toward the highest field strength will be precessing at a rate higher than those at the center. The protons in the material at a position toward the lowest field strength will be precessing at a rate lower than that at the center. All of this is happening at the same time and the signal from all of them will be received at the same time. The received signal will be the superposition of the signals of all of the rotating protons.

The local Larmor frequency at a point in the cylinder will be,

$$\omega\ z\ = \gamma B_0 + \gamma G_z z\ .$$

An MRI system will demodulate the signal that it acquires. This has the effect of subtracting the "carrier" frequency. Thus the resulting waveform will only have components due to the gradient, or,

$$\Omega\ z\ = \gamma G_z z$$

If the local spin density is $\rho\ z\ $, and the line element is dz, the contribution of that element to the measured signal will be,

$$ds = \rho\ z\ e^{i\gamma Gzt} dz\ .$$

The combined signal from all of the elements will be,

$$s = \int \rho\ z\ e^{i\gamma Gzt} dz\ .$$

With a little foreknowledge, we can define a reciprocal space number,

$$k = \gamma Gt\ ,$$

and come up with a function which represents all of the line elements of spin in a one dimensional sample,

$$s\ z\ = \int \rho\ z\ e^{ikz} dz\ .$$

Now, recall the definition of the Fourier Transform,

$$g(f) = \int_{-\infty}^{\infty} f(t) e^{-i2\pi ft} dt\ .$$

This function takes information in the time domain, and transforms it into the frequency domain. Its conjugate, the inverse Fourier Transform,

$$f(t) = \int_{-\infty}^{\infty} g(f) e^{i2\pi tf} df\ ,$$

takes information in the frequency domain and transforms it into the time domain. Our function describing the detected EMF of all of the spins in a sample certainly has the same form as an inverse Fourier transform. It is as if the signal acquisition has done this for us. This implies that we can reasonably take a Fourier transform of the signal and construct the frequency domain representation of that signal.

The result of a discrete Fourier transform will be to change the time-based source signal into a representation of the frequencies which compose that signal. The frequency

domain space is symmetrical, so a square wave input would result in a representation something like that shown in Figure 22. The lines are symmetrical to the right and the left of the origin, and represent the terms in the infinite series used to create the original wave. For example, the first line to the right of the origin represents $\sin(x)$ in the series. The second line represents $1/3\sin(3x)$, the third line represents $1/5\sin(5x)$ and so on.

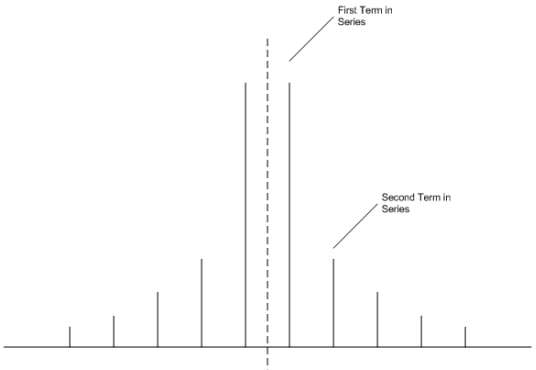

FIG 22: K-Space Representation of Square Wave

So the Fourier transform will discover all of the frequencies present in the measured signal.

Recall that the frequencies that will be found are generated by local spin densities which are precessing according to the local Larmor frequency. The local Larmor frequency is proportional to the gradient, which is in turn proportional to the position on the z-axis. The Fourier transform of the received signal is therefore a projection of the local spin densities onto the frequency domain, and the positions of those frequencies is a representation of the spatial locations of the local spin densities.

It may be easier to imagine this using a real world object – say a pencil. Figure 23 shows how this would work. The area toward the tip of the pencil is subjected to a higher magnetic field than the rest of the pencil due to an applied gradient. The Larmor frequency there will he higher. Any protons there will be precessing at a relatively higher frequency and will, after Fourier transforming the signal, have an associated frequency domain component projected onto the frequency domain representation shown below the pencil in the figure. The amplitude of the frequency domain representation corresponds to the strength of the signal at that frequency, and therefore directly to the number of protons at that location – the spin density.

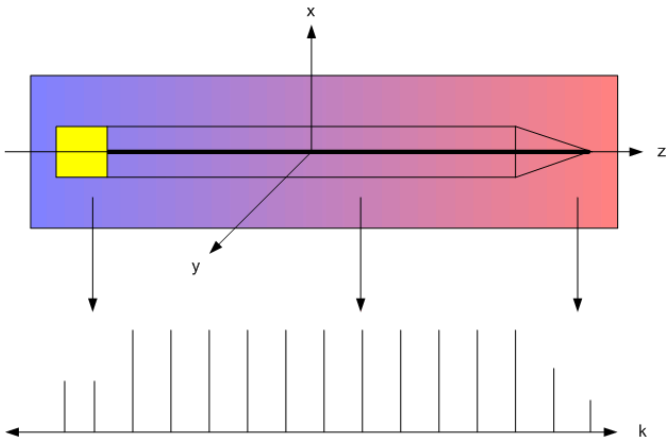

FIG 23: Projecting Precessions into the Frequency domain

Another point toward the center of the pencil will be exposed to a lesser field because of the gradient. Protons at that point will, therefore, be precessing at a lower frequency than the tip protons. Spins corresponding to this frequency will be projected onto frequency domain representation accordingly. Protons in the eraser section will have the lowest Larmor frequencies and will be reflected as a projection into the lowest frequency domain signals. Since the eraser is less dense than graphite, the amplitude of the frequency domain signal will be lower, reflecting that lower spin-density.

MRI images are generally shown in a grayscale format where a lighter gray corresponds to a higher spin density. Black corresponds to a zero spin density. The frequency domain representation of the pencil has higher spin densities represented as higher peaks in the signal.

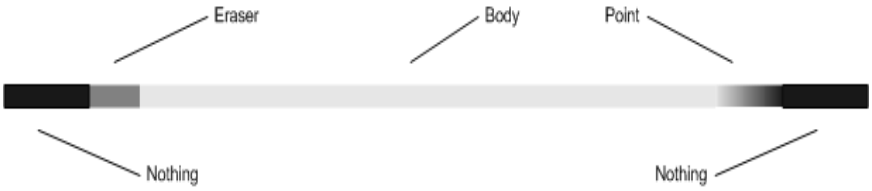

FIG 24: A 1-D MRI of a Pencil

Figure 24 shows what a 1-D MRI image of a pencil might look like. In this case, positions in the frequency domain correspond *directly* to the subject projection in real space. The pencil would be represented as a long gray line, representing the spin-density of the main body of the pencil, which tapers off to black at the point. The image fades to black at the tip because there is a descreasing amount of material containing fewer and fewer protons to contribute to the spin density. The lower spin density is represented as a darker image. The eraser would be seen as a darker rectangle also due to its reduced spin density (rubber being less dense than graphite), dropping immediately to a black area after the end of the eraser.

3.3 MULTIDIMENSIONAL MRI

The key mechanism which allows for extending 1-D MRI into two or more dimensions is the slice. In slicing, a gradient field is used to select a planar region of the subject for examination.

It does this selection by narrowing the region of resonance with the gradient field. If the dipole moment is precessing at a different rate than the rotating RF field, there can be no resonance, and the protons cannot absorb energy from the RF field. Remember that absorption of energy equivalent to $\omega\hbar$ where ω is the Larmor frequency was the underlying requirement for nuclear magnetic resonance. Figure 25 shows how a gradient field can be applied to select a perpendicular image slice.

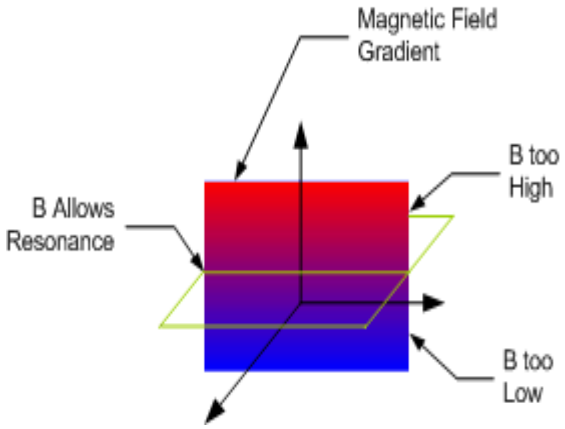

FIG 25: Slice Selection by Application of Magnetic Field Gradient

In order to select and measure a horizontal slice for an MRI scan, we need to combine several techniques. Figure 26 shows a sequence diagram representing such an image. We assume a static magnetic field is present, and therefore the magnetic moment is precessing tightly around the z-axis, which corresponds to the field direction. The slice selection gradient is switched on, which changes the Larmor frequency proportional to position. We would use a gradient on the z-axis to create an axial slice, for example (see Figure 3a).

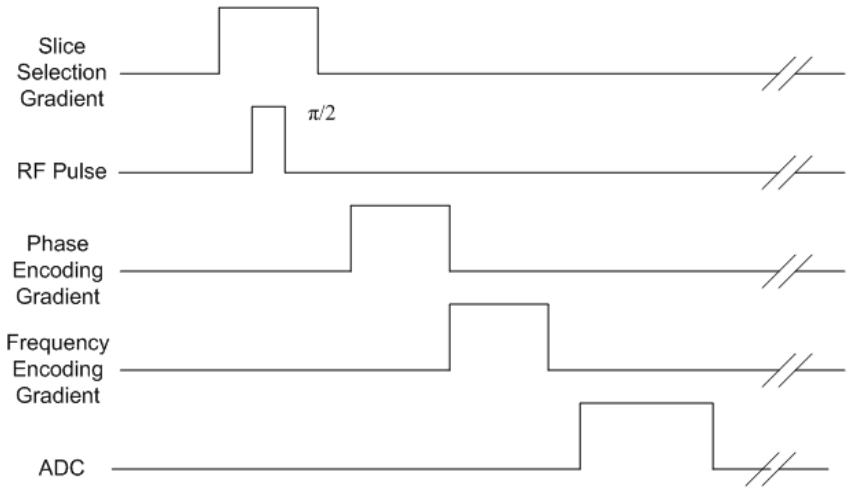

FIG 26: Sequence Diagram for Imaging

With the slice selection gradient in place, we apply the RF pulse at a frequency corresponding precisely to the Larmor Frequency at the slice location we have selected. The protons at this slice location find just the right amount of energy in the RF pulse and experience resonance. They rotate out of the z-axis and into the x-y axis in the case of the $\pi/2$ pulse. After the slice has been selected and the magnetic moment changed, a phase encoding gradient is enabled. In this case, it would be a gradient perpendicular to the z-axis, say the x-axis. A carefully selected gradient will cause protons at locations with higher field strengths to begin precessing faster than others in lower field strengths. Thus the phase of the protons in the higher field strengths will begin to lead that of the protons in the lesser field. This results in a phase difference to position mapping in the x-axis. After the phase encoding gradient, a frequency encoding gradient is applied along the remaining axis. This will have the effect of changing the frequency of precession of the protons proportional to position along the selected axis.

The final result of this manipulation is a plane of precessing protons, with position along one axis encoded by phase and the position along the other encoded by frequency. A measurement is then taken during which the combined signal is time sampled, digitized and stored as one element in a raw data array.

In order to construct an image, we need to repeat this measurement some number of times, changing the phase encoding gradient for each run. In order to understand why this is so, it is useful to consider a simple example.

Imagine a thin, square phantom[4] in which there is one volume element that has a non-zero nuclear spin, surrounded by a material with a zero nuclear spin. The goal is to image the single voxel with spin density.

[4] A phantom is a test target of known size and composition which is imaged by the MRI system.

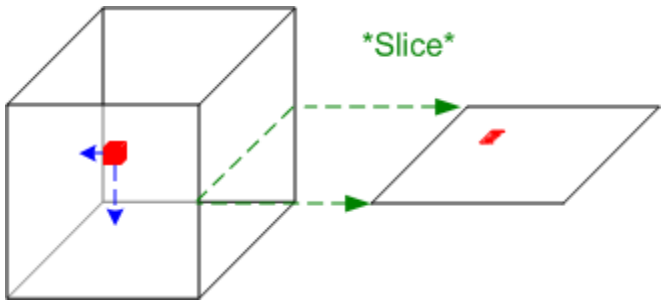

FIG 27: A Simple Hypothetical Phantom

Figure 27 shows what the phantom might look like, and shows how the slice selection gradient will select a plane of interest in the phantom. The only magnetic activity from the entire cube will be from the red area which is an area of a non-zero nuclear spin.

As described above, the MRI machine follows the sequence shown in Figure 26 a number of times, each time changing the phase encoding gradient. The number of separate phase measurements is selected to match the signal acquisition resolution and will produce a square raw data array. That is, if the signal sampled 256 times, we will need to perform 256 separate measurement passes to make the raw data array square.

The data collected from each measurement pass will show that the volume element has a particular frequency and phase associated with it. The square raw data array will reflect a selected plane within the phantom. Figure 28 shows what the data in the phase and time domain might look like. Note that there is one frequency of oscillation in the raw data, since the frequency encoding gradient does not change. The relative phase of the signal changes along the phase encoding direction (from bottom to top).

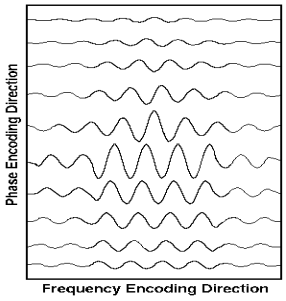

FIG 28: Illustration of Phase and Frequency Encoded Raw Data[5]

If we were to focus on one column of the raw data, we would see a signal constructed by the positions of the relative phases of the volume element. Note that by selecting the phase differences between runs, and sampling the signals vertically, we have synthesized another frequency. Figure 29 shows how this might look for the single voxel example.

[5] From http://www.cis.rit.edu/htbooks/mri/chap-7/chap-7.htm

Think about how a series of sine waves would look if they were stacked vertically and arranged slightly out of phase. This is shown in the red waves of Figure 29. If you follow the line drawn down through the waveforms, you can see that the amplitudes of the out of phase sine waves along that line will vary. The amplitudes along that line will vary as a sine wave.

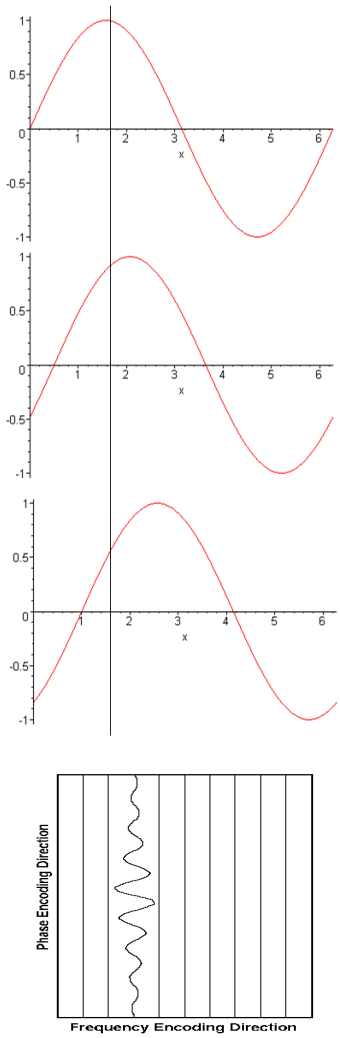

FIG 29: Illustration of one Column of Raw Data[6]

So, by varying the phase encoding gradient and taking multiple measurements, we have effectively created frequency components in the phase encoding direction which are encoded with position information along that axis.

In order to reconstruct the image, we would first perform a Fourier transform on the raw data in the frequency encoded direction. This would produce a frequency domain representation of the raw data. In the case of the single voxel example, it would produce a representation with a single frequency peak. The second step is to perform a Fourier

[6] From http://www.cis.rit.edu/htbooks/mri/chap-7/chap-7.htm

transform on the raw data in the phase encoded direction. This would produce another frequency domain representation of the raw data, but this time the frequencies are derived from sampling the phase differences. In our example, we would produce a representation with a single frequency peak.

These two frequency peaks correspond directly to the x and y position of the spin density in the phantom, and allow us to locate the spin density as shown in Figure 30.

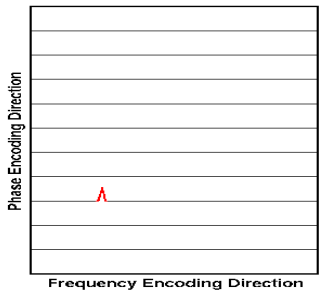

FIG 30: Locating the Spin Density in K-Space[7]

3.3 K-SPACE

In the MRI literature, you may see much discussion about k-space. K-space is interpreted as the place where the raw MRI signals are stored. In previous sections, we saw that the signal data looks like an inverse Fourier transform of the image. Position information is encoded in the phase and frequency of the signals which compose the data. The raw data representation of the subject is built up by taking a number of distinct measurements using differing phase encoding gradients. This process is called *traversing the k-space*.

Just as we can assign a gray scale to the spin densities of the Fourier transformed data and create an image of the subject, we can assign a gray scale to the digitized values in the raw data array and display an image of the k-space, as seen by the MRI machine.

Figure 31 shows an example of how this would look. Generally only the computer looks at the k-space image – people are interested in the real image that is reconstructed from the k-space data. It is interesting to have a peek at the k-space data, though.

[7] From http://www.cis.rit.edu/htbooks/mri/chap-7/chap-7.htm

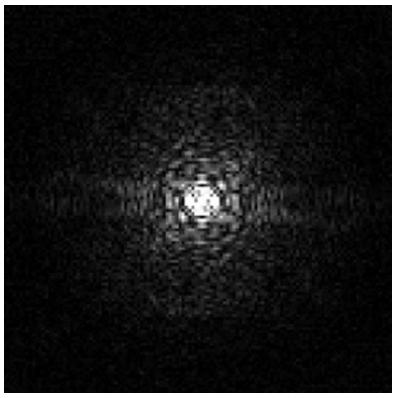

FIG 31: An Example of a K-Space Image (What is it?)

In Figure 31, the center of the image corresponds to the lowest frequencies. As you move radially outward from the center, you find higher and higher frequencies. Higher frequencies can be related back to the gradients used to encode the positions of the spins, but are also caused by edges in the spin densities. If there is a sharp change in spin densities, this will be reflected by the higher number of frequencies needed to represent that edge, just as one needs a large number of frequencies to accurately describe a square wave. Thus, contrast information in an MRI image is found at the center of the k-space image, and detail is found at the edges.

If we were to perform two Fourier transforms on the k-space data above in order to reconstruct the image, we would find the image shown in Figure 32.

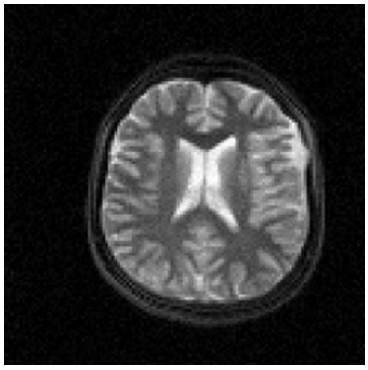

FIG 32: A Real Image Reconstructed from the K-Space Data

The k-space corresponds to the data that the MRI machine measures. It is a voltage versus time signal. The real space corresponds to the data that results from the Fourier transforms of the k-space signal. It is a spin density versus frequency signal. We tend to think of a Fourier transform as taking a voltage versus time (time domain) signal and mapping it into an amplitude versus frequency (frequency domain) signal. It can be somewhat confusing, but the k-space signal in MRI is taken over time, and the real space

signal is constructed over frequency. This is the opposite of what our intuition tells us. However, the terminology follows the applicability of the equations of the Fourier transforms instead of our intuition.

3.4 IMAGE QUALITY

The three primary contributors to perceived image quality are resolution, contrast and signal to noise ratio.

Two points in an image are said to be resolved if they can be distinguished. When two features on an image are distinguishable as separate, that image is said to posess higher resolution than one in which the features are indistinguishable.

It is clear that the number of data points in a given image affects the resolution; however that is true only up to a point. It turns out that the relaxation time of a sample also affects the resolution.

The MRI image can be thought of as a convolution of the spatial map of the spin densities and the spectral map. Convolution can be thought of as a smearing of one function by another. In a Fourier transform of a MRI image, the frequency peaks will have a FWHM[8] described by

$$\Gamma = \pi T_2^{*\ -1}.$$

This implies that as T_2^* increases, the width of the peaks will decrease. This is illustrated in Figure 33.

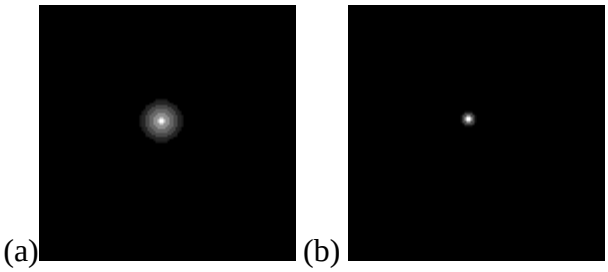

FIG 33: Images of Point Sources with Different Time Constants[9]
Image *a* corresponds to an image with short T_2^* and image b corresponds to a longer T_2^*.

Both images in Figure 33 were recorded with a pixel size much smaller than the resulting image. It is clear that there is a limiting value of resolution which depends on the combined relaxation time characteristics of the MRI system and the sample being imaged.

[8] Full Width at Half Maximum
[9] From http://www.cis.rit.edu/htbooks/mri/chap-7/chap-7.htm

In order to decide on an optimal pixel size for a particular system and sample we need to consider the frequency encoding gradient. The change in frequency over a sample based on an applied gradient field is,

$$\gamma B_g .$$

The amount of change per distance unit over the sample is then,

$$\gamma B_g^{-1}.$$

Taken together, this implies an optimal resolution for a given image,

$$\pi G \gamma T_2^{*-1}.$$

This produces enough pixels to resolve each frequency.

The second major component to perceived image quality is contrast. Since an MRI image is typically displayed in a grayscale, this implies that there must be enough gray levels to display the required information. This number should be high enough, but at some point, the difference between gray levels becomes imperceptible to the human eye. This is much like having "too much" pixel resolution as discussed previously. You don't want a situation where you have too few gray levels, but too many does you no good.

In order for there to be a perceived difference between tissues in an MRI image, there must be a difference in signal intensity, and this signal intensity must be displayed in a way to make it perceptible to a person.

Signal intensity in MRI is quantified by a number of *Signal Equations*. These equations describe the expected signal amplitude in the frequency domain spectrum for different measurement types. For example, the expected signal amplitude for a spin echo measurement is,

$$S = k\rho\left(1 - e^{-\frac{TR}{T_1}}\right)e^{-\frac{TE}{T_2}}$$

The signal is a function of several variables, called instrumental parameters

- k is a machine dependent variable specifying the gain of the hardware;
- T1, T2 and ρ are specific to a specific type of tissue;
- TR is the sequence repetition time (how quickly the measurement is repeated);
- TE is the echo time.

The variable which needs some comment here is TE. This is the time between the start of the RF pulse and its peak. The RF pulse actually has the form of a *sinc* pulse, shown in Figure 34.

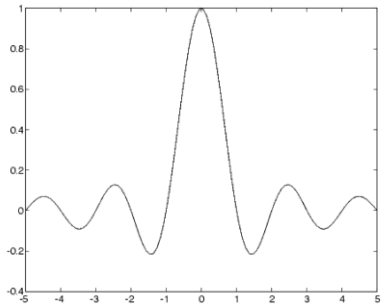

FIG 34: A sinc Pulse

The form of the sinc pulse corresponds to the function $\frac{\sin x}{x}$ and is the Fourier transform of the rectangle function, called the *boxcar* function in signal processing terminology. The parameter TE corresponds to the time between the start of the RF pulse to the peak of its associated sinc function.

The contrast between two tissues is defined as the difference between the signal amplitudes of the two signals as determined by the signal equations,

$$C_{AB} = |S_A - S_B|$$

The contrast of a particular MRI scan may be manipulated by changing the instrument parameters. Other instrumental parameters which are not discussed here are variables in other signal equations. These are,

- φ is the rotation angle. This is the angle through which the spin magnetic moments precess, controlled by the RF pulse (a π pulse, for example);
- TI is inversion time. This is related to sequences called Inversion Recovery sequences.

Figure 35 shows how changing the Echo Time (TE) affects the contrast of an image with TR held constant at 2 seconds. There is a fairly dramatic contrast change evident. From left to right, (35a-d) shows contrast at TE – 20, 40, 60 and 80 milliseconds).

a) 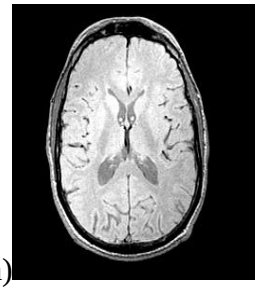 b) 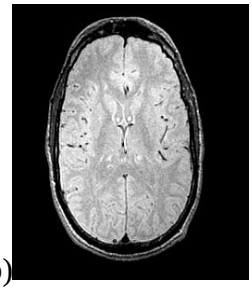 c) 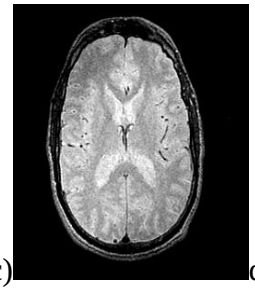 d) 

FIG 33: Contrast as Function of TE[10]

Signal to noise ratio is defined as the ratio of the average signal value for a particular type of tissue to the standard deviation of the noise in the image. The signal to noise ratio is improved by using image averaging.

In this process, a number of images are acquired and their average value is computed. Since noise is random, it tends to cancel itself out as the number of images is increased. The signals repeat across the various images so the contribution of the tissue response adds.

The number of images used duing the averaging process is known as Nex (the number of excitations). The signal to noise ratio is proportional to the square root of the number of excitations,

$$SNR \propto \sqrt{Nex}\ .$$

The results of averaging for a number of images can be seen in Figure 34. The image on the left is a sharpened single image. The image to the right is an average of 16 separate images sharpened to the same degree. There is a dramatic improvement in signal to noise ratio evident in the figure.

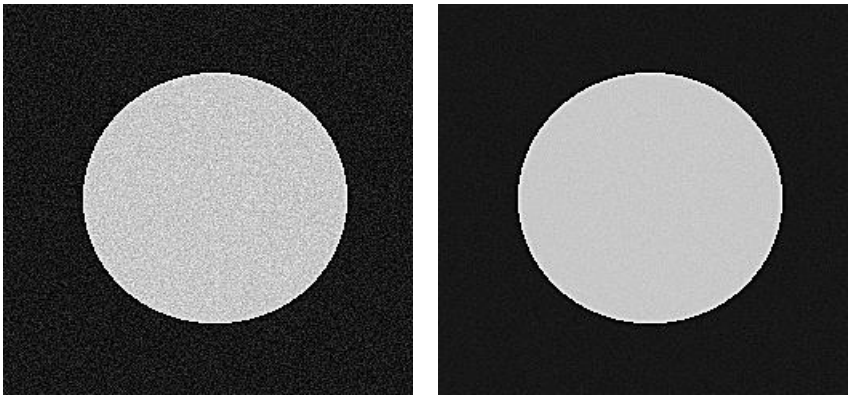

FIG 34: Signal to Noise Ratio Improvement by Averaging[11]

[10] From http://www.cis.rit.edu/htbooks/mri/chap-7/chap-7.htm
[11] From http://www.cis.rit.edu/htbooks/mri/chap-7/chap-7.htm

Generation of good tissue contrast in an MRI image depends on selecting appropriate pulse sequences for the types of tissues under investigation as well as the instrumental parameters. As many images as is feasible should be taken and median combined to increase the signal to noise ratio of the final image. The number of pixels in the image is generally fixed by the instrument manufacturer.

In situations where it is difficult to discriminate between tissues, it is possible to use *MRI Contrast Agents* to increase the difference in signal between the tissues.

3.5 ARTIFACTS

MRI Images can be affected by many things. One of the biggest culprits is metal. Metal creates large inhomogeneities in the external magnetic field. Figure 35 shows how a small metal clip in a woman's pony-tail elastic affected the MRI image of her head. This particular distortion is called "conehead," and the distorted head appearance was corrected by removing the pony elastic.

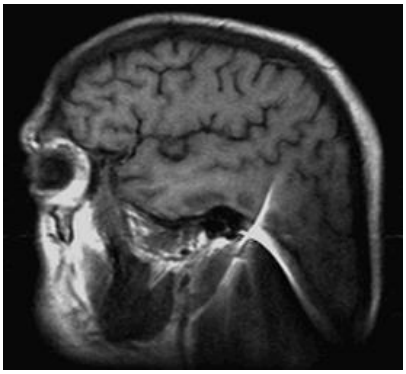

FIG 35: Conehead Artifact due to Metal in a Pony Elastic[12]

Sometimes artifacts are harder to correct. Figure 36 is an image with an artifact caused by dental work. Look closely. The subject really does not have a head shaped like an alien.

[12] Artifact images from http://wwwrad.pulmonary.ubc.ca/stpaulsstuff/MRartifacts.html

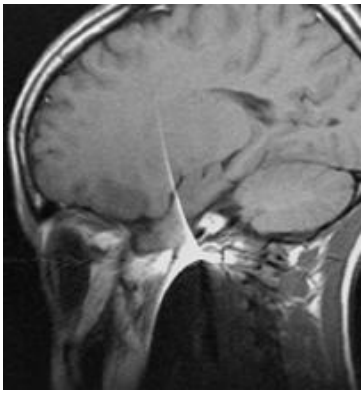

FIG 35: Artifact due to Patient Braces

Other artifacts are more subtle. For example, Moire fringes happen because of inhomogeneities in the static magnetic field. The resulting banding is shown in Figure 36.

FIG 36: Moire Fringes

An artifact due to the Gibbs phenomenon is shown in Figure 37. This artifact is caused by the finite number of encoding steps used in the Fourier transform to recreate the image. It really does take an infinite number of sine waves to reconstruct a square wave.

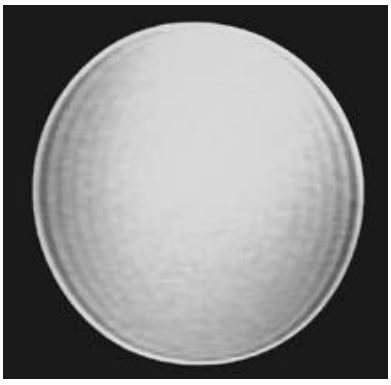

FIG 37: Truncation Artifact

There are a large number of recognized artifacts which may appear in MRI images. They can range from the humorous (conehead) to the tragic (mistaking an entry slice artifact for a blood clot and scheduling emergency surgery).

It is the responsibility of the radiologist to understand the underlying technology well enough to generate a good image and correctly interpret the results.

4.0 SUMMARY

The field of Nuclear Magnetic Resonance and MRI is incredibly rich in almost any dimension one could imagine. The fact that the field of MRI even exists is a testament to human determination and creativity

From its humble beginnings in 1946, the various applications of NMR have been taken to incredible lengths. We can use NMR spectroscopy to understand the three-dimensional structure of chemicals. NMR microscopy, which is a high spatial resolution version of MRI, is allowing studies of chemical processes in single cells down to the scale of a micrometer. Nuclear Magnetic Resonance has applications in fields as diverse as biology, materials science, chemical physics, petrochemicals, food processing, polymers and, of course, medicine.

The physics of Nuclear Magnetic Resonance is deceptively simple, but the solutions to the related scientific and engineering problems are fiendishly clever.

There are many World-Wide-Web resources available on the subject of Nuclear Magnetic Resonance, and especially MRI. Here are some recommendations:

- The Basics of MRI, Joseph Hornak
  - Book on MRI accessible on the web
  - http://www.cis.rit.edu/htbooks/mri/
- 1D NMR Basics, Nikolai Shokhirev
  - Tutorial on NMR
  - http://www.shokhirev.com/nikolai/abc/nmrtut/NMRtut1.html
- Magnetic Resonance Imaging, HyperPhysics
  - Online Physics Encyclopedia Article
  - http://230nsc1.phy-astr.gsu.edu/hbase/nuclear/mri.html
- Nuclear Magnetic Resonance, Wikipedia
  - Free Encyclopedia Article
  - http://en.wikipedia.org/wiki/Nuclear_magnetic_resonance
- How MRI Works, HowStuffWorks
  - http://www.howstuffworks.com/mri.htm

Of course, a web search engine will return an almost endless supply of information about MRI from any imaginable perspective.

Refereneces

[1] Fukushima E, Roeder S., Experimental Pulse NMR A Nuts and Bolts Approach, Addison-Wesley, Reading (1981)

[2] Griffiths D., Introduction to Electrodynamics, Prentice Hall, Upper Saddle River (1999)

[3] Griffiths D., Introduction to Quantum Mechanics, Prentice Hall, Upper Saddle River (2005)

[4] Haacke M., et al., Magnetic Resonance Imaging: Physical Principles and Sequence Design, Wiley-Liss, New York (1999)

[5] Hahn E., Free Nuclear Induction, Physics Today, Nov 1953.

[6] Resnick R., Halliday D., Krane K., Physics Volume One, John Wiley and Sons, New York (2002)

[7] Resnick R., Halliday D., Krane K., Physics Volume Two, John Wiley and Sons, New York (2002)

[8] Slichter C., Principles of Magnetic Resonance with Examples from Solid State Physics, Harper and Row, New York (1963)